



HAL
open science

**Effect of the three-dimensional microstructure on the normal incidence sound absorption coefficient of foams:
A parametric study**

Fabien Chevillotte, Camille Perrot

► **To cite this version:**

Fabien Chevillotte, Camille Perrot. Effect of the three-dimensional microstructure on the normal incidence sound absorption coefficient of foams: A parametric study. 22nd International Congress on Acoustics (ICA 2016), Sep 2016, Buenos Aires, Argentina. hal-01664290

HAL Id: hal-01664290

<https://hal.science/hal-01664290>

Submitted on 14 Dec 2017

HAL is a multi-disciplinary open access archive for the deposit and dissemination of scientific research documents, whether they are published or not. The documents may come from teaching and research institutions in France or abroad, or from public or private research centers.

L'archive ouverte pluridisciplinaire **HAL**, est destinée au dépôt et à la diffusion de documents scientifiques de niveau recherche, publiés ou non, émanant des établissements d'enseignement et de recherche français ou étrangers, des laboratoires publics ou privés.

Materials for Noise Control: Paper ICA2016-589**Effect of the three-dimensional microstructure on the normal incidence sound absorption coefficient of foams: A parametric study****Chevillotte Fabien^(a), Perrot Camille^(b)**^(a) Matelys, Vaulx-en-Velin, France, Fabien.chevillotte@matelys.com^(b) Université Paris-Est, Marne-La-Vallée, France, camille.perrot@u-pem.fr**Abstract**

Sound absorption arises mainly from visco-thermal dissipation of a pressure wave propagating through a porous material. First-principal calculations and X-ray computed tomography experiments reveal that the sound absorbing behavior of real foam samples made from dispersion of gas bubbles in liquid matrices can be directly described from a simple three-dimensional regular model of hollow spheres, which opens new avenues for optimal design of acoustic materials. However, the proper choice of bubble and interconnection sizes, two critical parameters of the foam's morphology, depend on the sample thickness, the frequency range of interest (the choice of the optimization criterion), and the kind of excitation (normal or diffuse incidence). This presents a problem: a small interconnection combined with large pores is necessary for thin sample thicknesses in order to provide a resistive and tortuous layer of porous sample, but interconnections have to be larger and pores smaller for thicker samples to be able to dissipate viscous energy in all the thickness of the material by avoiding an excess of reflected waves. Moreover, the manufacturing process places constraints on the accessible range of porosities and pore radius. The selected criterion is a sound absorption average over third octave bands between 125 Hz and 4000 Hz. In this communication, massive computations are therefore used to provide guidelines for selecting the appropriate foam's morphology. This study is restricted to normal incidence.

Keywords: Engineered foams, tunable acoustic properties.

Effect of the three-dimensional microstructure on the normal incidence sound absorption coefficient of foams: A parametric study

1 Introduction

The acoustical macro-behavior has been modeled from microstructure for a wide range of materials: nickel hollow spheres packings [1], open-cell aluminum foams [2], perforated closed-cell metallic foams [3], lead shot and expanded perlite [4], polyurethane foams [5] and gypsum foams [6].

Also, most of the published works relates to the identification of microstructural models allowing to capture the main dissipation mechanisms. These latter works do not include the corresponding parametric study which could lead to an effective improvement of the functional properties. Although it has been shown that two-dimensional microstructural models can provide a qualitative insight in the effect of the morphological modifications on transport properties to understand the sound absorption mechanism [7], three-dimensional results directly applicable to real foam samples are still missing to provide quantitative guidelines for manufacturers.

Moreover, the manufacturing process places constraints on the accessible range of porosities and microscopic parameters (pore size, throat size). This implies that large computational facilities could be used to provide guidelines for selecting the appropriate foam morphology.

The three-dimensional idealized periodic microstructural model studied in this paper represents a large class of cellular solid foams whose transport properties are of scientific and technological interest. A parametric study is carried out by using this geometrical model to develop a quantitative understanding between pore structure and sound absorbing properties. Here, the normal incidence (NI) acoustical excitation is considered. It is therefore possible to test and compare the simulation results with the physical assumptions corresponding to an impedance tube laboratory measurement. A systematic application of the model to open-cell foams with porosity - lying in the range 0.7 to 0.99 yields quantitative results linking simple geometrical descriptors like the pore radius R_p and the throat radius R_t (i.e., the radius of the narrowest part interconnecting the pore space) with effective transport and sound absorbing properties for various sample thicknesses in NI. This approach also tends to provide information relative to the effect of the manufacturing process variability on the performance of the product.

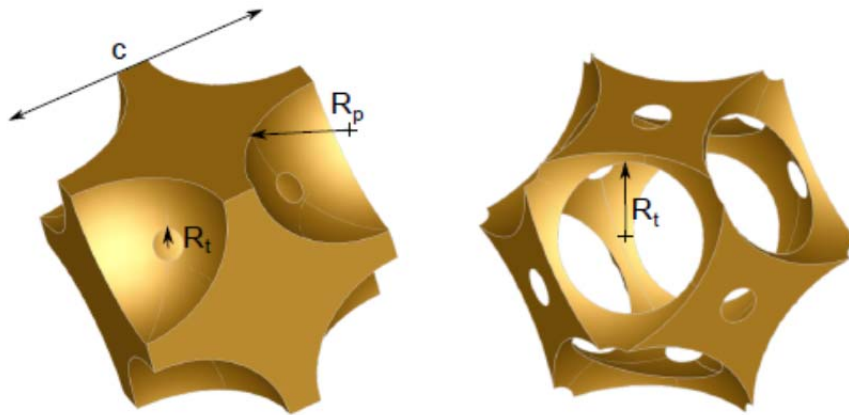


Figure 1: Illustration of cells: Porosity $\phi = 0.7$ (left), Porosity $\phi = 0.96$ (right)

2 Methodology

2.1 Hybrid micro-macro method

Contrary to the direct approach which solves the linearized Navier-Stokes and the heat equations in harmonic regime, the hybrid method relies on approximate but robust semi-phenomenological models [Johnson-Champoux-Allard (JCA), Johnson-Champoux-Allard-Lafarge (JCAL)]. By considering a rigid porous sample saturated by a Newtonian fluid, Johnson *et al.*[8] derived a simple yet robust description of frequency-dependent modeling of the visco-inertial effects from macroscopic parameters. Similarly, Champoux and Allard [9] derived a similar response function of the thermal effects. Lafarge *et al.* [10] improved the frequency-dependence description of the thermal response function and unified both of these descriptions. A synthesis of JCA and JCAL models can be found in [11]. These models are attractive due to their ability to avoid computing numerically the solution of the full frequency range values of the effective density/bulk modulus. The principle is to solve the local equations governing the asymptotic frequency-dependent visco-thermal dissipation phenomena at the microscopic scale. All the macroscopic parameters of interest can be determined from only three asymptotic calculations:

The open porosity ϕ is defined as the fraction of the interconnected pore fluid volume to the total bulk volume of the porous aggregate. A second parameter which is widely used to characterize the macroscopic geometry of porous media is the hydraulic radius, defined as twice the ratio of the total pore volume to its surface area. This characteristic length may also be referred to as the thermal characteristic length Λ' in the context of sound absorbing materials [9]. Both of these parameters are estimated by direct spatial integration on the volume and surface elements of the microstructure.

The static air flow resistivity σ (or static viscous permeability $k_0 = \eta/\sigma$, where η is the dynamic fluid viscosity) is computed from the Stokes problem [12]. The static viscous tortuosity α_0 , another transport parameter significant of the viscous flow, might also be computed from the same boundary value problem. This last parameter is not used in this study.

The viscous characteristic length Λ and the high frequency limit of the tortuosity α_{∞} are calculated using a perfect (nonviscous) incompressible fluid which formally behaves according to the electric conduction [13]. They are determined from solutions of the Laplace's equation. Λ should be interpreted as a weighted volume-to-surface ratio accounting for the throat region.

The static thermal permeability k_0' , also known as the inverse of the trapping constant τ in the context of physical chemistry - where surface exchanges play an important role - was computed by means of thermal conduction problem where the solid skeleton is considered as a thermostat. There is a formal analogy with diffusion-controlled reactions [14]. An additional macroscopic parameter, the static thermal tortuosity α_0' , might be derived from the same boundary value problem.

2.2 Selection of the representative cell

There are numerous foaming processes but the principle is always to make growing gas bubbles within a liquid matrix. In three dimensions, the most simple idealized cell is a regular positioning of spheres with identical sizes. According to the geometric modeling adopted, growing bubbles will tend to interconnect pores and create a network of open pores. The physics of foams suggests that the body-centered cubic (BCC) arrangement (see Fig. 1) is the most appropriate since it tends to the Kelvin cell (tetrakaidecahedron) when pores are growing (see Fig. 1 (right)). The Kelvin cell is well known for modeling high porosity foams as polyurethane or polymer foams [15].

2.3 Selection of the evaluation criterion

When dealing with a parametric study, the selection of the evaluation criterion is of great importance.

The single number rating w is commonly used in European countries (ISO 11654) for ranking the sound absorption performances of materials when submitted to a diffuse field excitation. This indicator is the value of the reference curve at 500 Hz after translation according to ISO 11654 [16].

Two other single number ratings are commonly used, the sound absorption average (SAA) and the noise reduction coefficient (NRC). The SAA is the average, rounded off to the nearest 0.01, of sound absorption coefficients of a material for the twelve one-third octave bands from 200 through 2500 Hz [17].

The NRC is the rounded average of the sound absorption coefficient for the four octave bands from 250 to 2000 Hz rounded to the nearest multiple of 0.05.

The selected criterion is a sound absorption average over third octave bands between 125 and 4000 Hz ($SAA_{125-4000}$) to enlarge the frequency range of interest. The use of the log scale enables to increase the weight of the low frequencies. Here, the parametric study is based on this criterion with a focus on NI acoustical excitation.

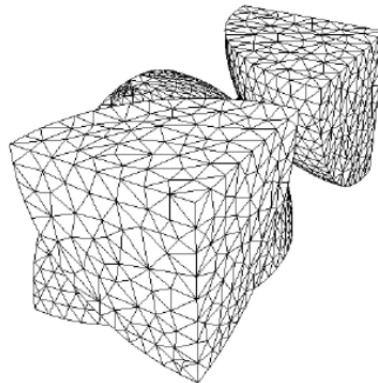


Figure 2: Example of mesh: $N = 20$, $Q_{\max} = 2$. By using some symmetries of the geometry and the excitation, the computations can be carried out on one-quarter of a single unit cell.

3 Parametric study

3.1 Mesh sensitivity analysis

A sensitivity analysis is conducted to check the robustness of the numerical method and to ensure that the parametric study is exploitable. The considered cell is a body centered cubic (BCC) packing with a pore radius R_p of 230 μm , a throat (or window) radius R_t of 55 μm and a target porosity ϕ_t of 0.7. The mesh can be refined by increasing the number of elements (N) per unit length or by increasing the quality of tetrahedrons. The quality factor Q is defined as the ratio of the inscribed sphere radius to minimum edge length. The lower is this factor, the better is the quality of the element. An example of mesh is given in Fig. 2. The mesh sensitivity analysis was also compared to a small variation of the throat size, which is a first order local geometry parameter for predicting the acoustical macro-behavior of porous media.

We found that the macroscopic parameters vary only slightly with typical meshing parameters (less than 1%). By contrast, the effect of a small variation of the throat size on the same macroscopic parameters was more significant, indicating that the convergence of the solution is ensured.

Indeed, a variation of 1 μm (1.8 %) of the throat radius implies a variation of the same order of magnitude on the viscous characteristic length Λ and on the low and high frequency limits of the tortuosity α_0 and α_∞ . Meanwhile, a variation around 5% is observed on the air flow resistivity (and the static viscous permeability which is inversely proportional to the static air flow resistivity). This result is consistent with the fact that, for mono-disperse packings, the static air flow resistivity is inversely proportional to the square of throat size

The main result of this study is that a small variation of the throat size corresponds to a variation of the macroscopic parameters higher than the error due to the mesh quality.

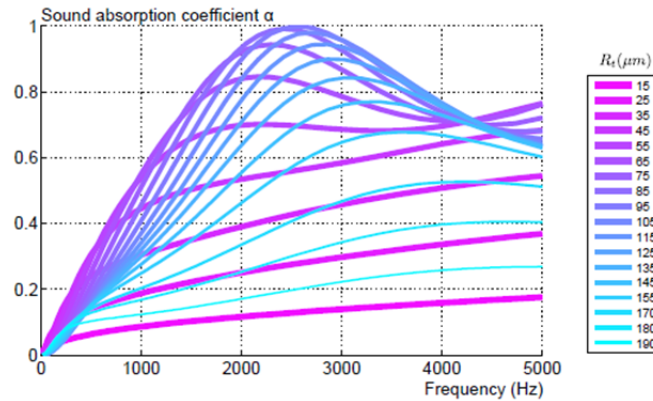


Figure 3: Effect of the throat size on the sound absorption coefficient (normal incidence). 25 mm thick sample with a rigid backing.

3.2 Effect of the throat size

After analyzing the mesh sensitivity, this study is focused on the effect of the throat size on the macroscopical behavior of the material. The throat size is known to be the main parameter governing the acoustical behavior of the materials. This microscopic parameter governs the static air flow resistivity, which in turns controls the overall absorption level.

The BCC cell is used with a pore radius of 230 μm . The sample thickness L is 25 mm. The throat radius R_t is varied from 10 μm to 195 μm . The influence of the throat size on the sound absorption coefficient is shown in Fig. 3 for NI excitation.

Based on our simulation data, it can be shown that the static air flow resistivity σ is largely decreasing while the throat size is increasing. The high frequency limit of the tortuosity α_∞ is strongly decreasing as the ratio R_p/R_t is approaching unity. Except in the vicinity of the previously mentioned limit, the viscous characteristic length Λ adopts a value generally close to the one of the throat radius R_t . These results are consistent with what can be found in the literature for mono-disperse packings.

Moreover, a specific throat radius can be found for each sample thickness. Importantly, the specific throat radii are increasing with the sample thickness. This increase looks like a function of the square root of the sample thickness \sqrt{L} . Previous works on perforated solid [3] and plates [18] have shown this trend. The thicker is the sample, the higher is the tolerance on the throat size (not shown here).

3.3 Effect of pore size

The second part of this parametric study is focused on the pore size effect. The sample thickness is 25 mm with a rigid backing and the initial configuration is the specific one as mentioned in the previous section ($R_p = 230 \mu\text{m}$, $R_t = 60 \mu\text{m}$, $SAA^{NI} 125-4000 \approx 42\%$). In this study, the pore radius is varied from 80 to 490 μm .

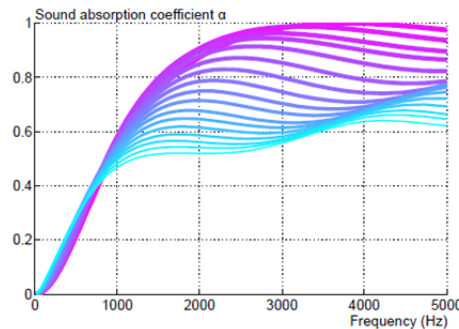


Figure 4: Effect of the pore size on the sound absorption coefficient (normal incidence). 25 mm thick sample, rigid backing.

The influence of the pore size on the sound absorption coefficient is shown in Fig. 4 for NI excitation. It can be seen that the influence of the pore size has a lower influence on the overall sound absorption coefficient than the throat size. In other words, the performance criterion is less sensitive to a variation of the pore size in comparison to a variation of the throat size.

Importantly, the ratio between the thermal and the viscous characteristic lengths was found to be not constant, nor equal to three. Therefore, the hypothesis of a constant Λ'/Λ ratio cannot be made for an accurate characterization of real foam samples by using inversion protocols, especially when structural information on the pore and throat size radii is unavailable.

Besides, a specific pore radius can be found for each sample thickness and for each excitation. In contrast to the result on specific throat radii, the specific pore radii are clearly decreasing with the sample thickness. This result can be explained by the fact that thin samples require a high tortuosity in order to improve the sound absorption. Indeed, a higher tortuosity value is obtained by increasing the ratio $R_p=R_t$. This characteristic feature may strong implications on the manufacturing process, especially if one thinks that the phenomenon referred to as "drift" is a normal characteristic of an industry. Indeed, the relative variation of the criterion for the pore size is smaller than the relative variation of the criterion for the throat size.

3.4 Multi-parameter analysis

The influence of the throat size and the pore size have been independently studied in the previous sections. A full parametric study over ϕ , R_p and L is carried in this section.

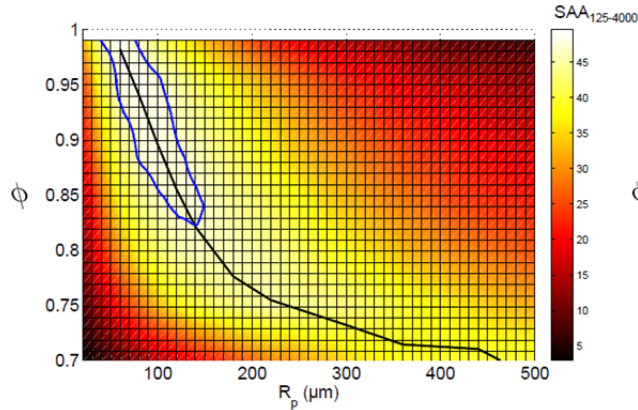


Figure 5: Effect of the open porosity ϕ and pore size R_p on the sound absorption criterion (normal incidence). 25 mm thick sample.

The resultant two-dimensional maps and the corresponding $SAA_{125-4000}$ criterion are presented in Fig. 5 for the NI with a thickness of 25 mm. The thick line shows the morphological configurations maximizing the sound absorption criterion ($SAA_{125-4000}$). The contours enabling 95 % of the maximum performance are also shown in these maps.

Knowing the pore size R_p and the cell size c of the BCC cell, the throat size R_t can be calculated for each configuration following this formula (Fig. 1):

$$R_t = \sqrt{R_p^2 - \left(c \frac{\sqrt{3}}{4}\right)^2} \quad (1)$$

The microscopic and the macroscopic parameters are given as a function of the open porosity for configurations maximizing the sound absorption average in Fig. 6 (this corresponds to the

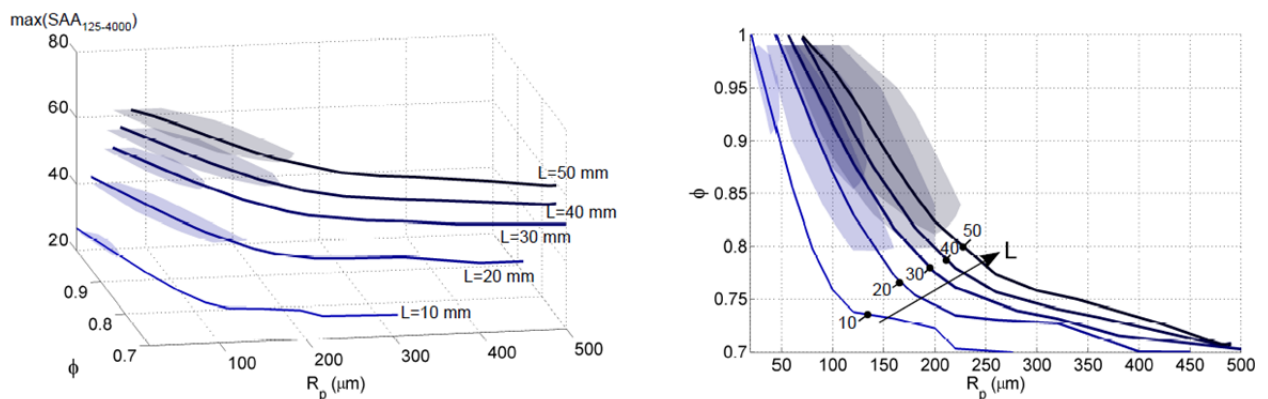


Figure 6: Effect of the open porosity ϕ and pore size R_p on the sound absorption criterion for various sample thicknesses with normal incidence excitation (Left: 3D, Right: 2D).

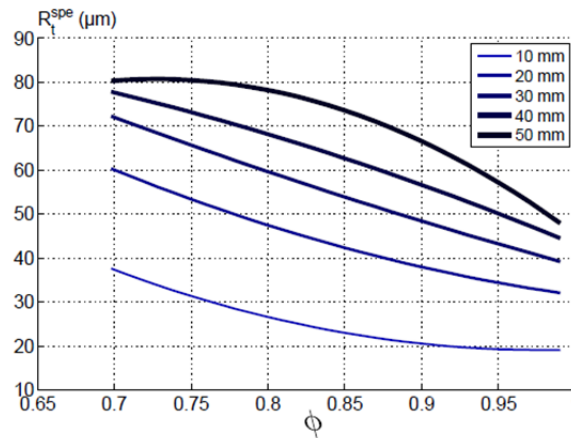


Figure 7: Specific throat radii as a function of the open porosity for various sample thicknesses (normal incidence).

variation of parameters along the thick line.). The sound absorption average appears to be nearly constant for porosities higher than 0.75. Indeed, the criterion slightly increases from 53% at $\phi = 0.75$ to 56% at $\phi = 0.99$. Meanwhile, the pore size R_p largely decreases while the throat size R_t decreases as the porosity ϕ increases. Clearly, the ratio R_p/R_t and thus the high frequency limit of the tortuosity α_∞ decrease. The calculated configurations maximizing the sound absorption criterion ($SAA_{125-4000}$) for thicknesses between 10 and 50 mm are also given for the normal incidence excitation (see Fig. 6). The zones having a criterion higher than 95% of the maximum sound absorption average are also illustrated for each thickness. The value of 95% is taken for each thickness using the reference of the maximum sound absorption average for the considered thickness.

Finally, the corresponding specific throat radii, maximizing the sound absorption criterion, are plotted as a function of the open porosity for thicknesses between 10 and 50 mm for NI excitation in Fig. 6.

In agreement with what has previously been observed with a low porosity system at $\phi = 0.7$ throughout Sec. III.B, the reported specific throat radii are increasing with the sample thicknesses whatever the considered range of open porosities [0.7-0.99]. More thorough discussions of the utility of this graph will be given in the next section using practical examples.

4 Practical examples

The melamine foam, known as a good sound absorber, with parameters $\phi = 0.99$, $R_p \approx 100 \mu\text{m}$, $R_t \approx 50 \mu\text{m}$ is well identified in the zone maximizing the sound absorption average for thicknesses higher than 30 mm in Figs. 6. In contrast, the maximum in sound absorption for open cell foams that have a thickness in the vicinity of 10 mm is directly linked to microstructural characteristic lengths that must be smaller. As it can be seen from Figs. 6 and 7, an improvement of the sound absorption is expected for a structure as defined by a combined reduction of the pore and throat sizes ($R_p \approx 40 \mu\text{m}$, $R_t \approx 20 \mu\text{m}$).

The second example is provided by a foam manufactured such that the following parameters are obtained: $\phi = 0.85$, $R_p = 150 \mu\text{m}$ and $L = 20 \text{ mm}$. An analysis of the data reported here reveals that there are three means to improve the sound absorption of this foam:

The simplest way to improve the sound absorption properties of this foam is to provide it into the thickness corresponding to the best achieved criterion at a given pore radius. It is shown in Figs. 4 that this kind of foam should be used with a thickness of 40 mm when a NI excitation is considered.

Finally, the porosity could be reduced to $\phi = 0.75$ to improve the sound absorption while keeping the thickness of 20 mm and the pore size $R_p = 150 \mu\text{m}$.

5 Conclusion

The computations of transport and sound absorbing properties of three-dimensional open cell foams combined with systematic modifications of their local characteristic sizes could lead to new insights on the morphologies to be obtained in order to achieve the maximal performance.

As a first step along these lines, we further analyzed the effect of the throat size on the macroscopic parameters governing sound absorption (Fig. 3). The numerical estimates of the transport and sound absorbing properties obtained from a three-dimensional model in a bottom-up approach produced results which can be used to simultaneously follow the evolution of macroscopic parameters with the throat size variations (detailed data not reported here). The throat size is the key morphological parameter for controlling the sound absorption (Figs. 3 and 4).

The generalization of these calculations at different sample thicknesses also revealed that the optimal throat size increases with the sample thickness of the porous material. Because the specific throat radii tolerance maximizing the sound absorption average increases while increasing sample thickness, this also suggests that applications targeting small sample thicknesses require a more elaborated control of the manufacturing process due to the drift phenomenon.

Controlling pore and throat size modifications is a useful strategy for engineering the sound absorption spectrum of an open cell foam. However, the emphasis here is on the different possible strategies leading to a significantly enhanced sound absorption average at NI ($SAA_{125-4000}$). Indeed, the effects of the pore size modifications discussed above (Fig. 4) can be seen as a supplementary morphological parameter along with the throat size, the porosity, and the sample thickness of the foam to map the typical features of the porous medium (Fig. 5). The successful bottom-up elaboration of morphologically precise open cell foams opens extensive opportunities for the analysis of their transport and sound absorbing properties (see Sec. IV for practical examples) and for the manufacturing of porous samples with enhanced performances by following the guidelines provided all along this paper (Figs. 6, 7).

References

- [1] Gasser, S.; Paun, F, Bréchet, Y. Absorptive properties of rigid porous media: Application to face centered cubic sphere packing, *J. Acoust. Soc. Am.*, 117 (4), 2005, 2090-2099.
- [2] C. Perrot, F. Chevillotte, R. Panneton, "Dynamic viscous permeability of an open-cell aluminum foam: Computations versus experiments", *J. App. Phys.* 103, 024909 (2008).
- [3] F. Chevillotte, C. Perrot, R. Panneton, "Microstructure based model for sound absorption predictions of perforated closed-cell metallic foams", *J. Acoust. Soc. Am.* 128 (4), 1766-1776 (2010).
- [4] R. Venegas, O. Umnova, "Acoustical properties of double porosity granular materials", *J. Acoust. Soc. Am.* 130 (5), 2765-2776 (2011).
- [5] C. Perrot, F. Chevillotte, M.T. Hoang, G. Bonnet, F.-X. Bécot, L. Gautron, A. Duval, "Microstructure, transport, and acoustic properties of open-cell foam samples: Experiments and three-dimensional numerical simulations", *J. Appl. Phys.* 111, 014911 (2012).
- [6] F. Chevillotte, C. Perrot, E. Guillon, "A direct link between microstructure and acoustical macro-behavior of real double porosity foams", *J. Acoust. Soc. Am.* 134 (6), 4681-4690 (2013).
- [7] C. Perrot, F. Chevillotte, R. Panneton, "Bottom-up approach for microstructure optimization of sound absorbing materials", *J. Acous. Soc. Am.* 124 (2), 940- 948 (2008).
- [8] D.L. Johnson, J. Koplik, and R. Dashen, "Theory of dynamic permeability and tortuosity in fluid-saturated porous media", *J. Fluid Mech.*, 379-402 (1987).
- [9] Y. Champoux and J.F. Allard, "Dynamic tortuosity and bulk modulus in air-saturated porous media", *J. Appl. Phys.* 70, 1975-1979 (1991).
- [10] D. Lafarge, P. Lemarinier, J.F. Allard, and V. Tarnow, "Dynamic compressibility of air in porous structures at audible frequencies", *J. Acoust. Soc. Am.* 102, 1995-2006 (1997).
- [11] J.F. Allard, N. Atalla, *Propagation of sound in porous media. Modeling sound absorbing materials* (Wiley, Chichester, UK, 2009, 2nd Ed.) Chap 5, 358 pages.
- [12] J.-L. Auriault, C. Boutin, and C. Geindreau, *Homogenization of Coupled Phenomena in Heterogeneous Media* (Wiley-ISTE, London, UK, 2009), pp. 197-226.
- [13] R.J.S. Brown, "Connection between formation factor for electrical resistivity and fluid-solid coupling factor in Biot's equations for acoustic waves in fluid-filled porous media," *Geophysics* 45, 12-69 (1980).
- [14] J. Rubinstein, S. Torquato, "Diffusion-controlled reactions: Mathematical formulation, variational principles, and rigorous bounds", *J. Chem. Phys.* 88, 63-72 (1988).
- [15] D. Weaire and S. Hutzler. *The Physics of Foams*, (Oxford University Press, Oxford, 1999), 264 pages.
- [16] ISO 11654, "Acoustics - Sound absorbers for use in buildings - Rating of sound absorption", (1997).
- [17] ASTM C423, "Standard Test Method for Sound Absorption and Sound Absorption Coefficients by the Reverberation Room Method," (2002).
- [18] F. Chevillotte, "Controlling sound absorption by an upstream resistive layer", *Applied Acoustics* 73, 56-60 (2012).